Title	Tunneling-induced angular momentum for single cold atoms
Authors	Menchon-Enrich, R.;McEndoo, Suzanne;Mompart, J.;Ahufinger, V.;Busch, Thomas
Publication date	2014
Original Citation	Menchon-Enrich, R., McEndoo, S., Mompart, J., Ahufinger, V. and Busch, T. (2014) 'Tunneling-induced angular momentum for single cold atoms', Physical Review A, 89(1), 013626. (5pp). doi:10.1103/PhysRevA.89.013626
Type of publication	Article (peer-reviewed)
Link to publisher's version	https://journals.aps.org/pra/abstract/10.1103/PhysRevA.89.013626 - 10.1103/PhysRevA.89.013626
Rights	© 2014, American Physical Society
Download date	2024-05-05 11:32:51
Item downloaded from	https://hdl.handle.net/10468/4482

University College Cork, Ireland
Coláiste na hOllscoile Corcaigh

Tunneling-induced angular momentum for single cold atoms

R. Menchon-Enrich,[1] S. McEndoo,[2] J. Mompart,[1] V. Ahufinger,[1] and Th. Busch[3,4]

[1]*Departament de Física, Universitat Autònoma de Barcelona, E-08193 Bellaterra, Spain*
[2]*SUPA, Physics, Engineering & Physical Sciences, Heriot-Watt University, Edinburgh EH14 4AS, Scotland, United Kingdom*
[3]*Physics Department, University College Cork, Cork, Ireland*
[4]*Quantum Systems Unit, OIST Graduate University, Okinawa 904-0495, Japan*

We study the generation of angular momentum carrying states for a single cold particle by breaking the symmetry of a spatial adiabatic passage process in a two-dimensional system consisting of three harmonic potential wells. By following a superposition of two eigenstates of the system, a single cold particle is completely transferred to the degenerate first excited states of the final trap, which are resonantly coupled via tunneling to the ground states of the initial and middle traps. Depending on the total time of the process, angular momentum is generated in the final trap, with values that oscillate between $\pm\hbar$. This process is discussed in terms of the asymptotic eigenstates of the individual wells and the results are checked by simulations of the full two-dimensional Schrödinger equation.

I. INTRODUCTION

Controlling the states of quantum particles is a challenging task and a topic of significant present activity in the fields of atom optics, quantum computation, quantum metrology, and quantum simulation of condensed matter systems [1]. In particular, the generation of angular momentum for matter waves is attracting much attention, for instance, in studying superfluid properties of Bose-Einstein condensates (BECs) [2]. These condensates can sustain vortices, which have been envisioned to be used in applications for interferometry, for example, gyroscopy with counterrotating vortex superpositions [3], for quantum information, such as coherent superpositions of arbitrary winding numbers [4], or entangled vortex states [5], and as a way to study the behavior of random polynomial roots [6]. Different techniques have been proposed and experimentally reported to generate angular momentum with single atoms and BECs, such as stirring with a laser beam [7], phase imprinting [8], transfer of orbital angular momentum from optical states [9,10], rotating traps [2,11], turbulence [12], dynamical instabilities [13], or merging multiple trapped BECs [14].

At the same time, adiabatic techniques to control the external degrees of freedom of massive particles have been developed [15], based on the spatial analog of the stimulated Raman adiabatic passage (STIRAP) technique [16]. For the center-of-mass degree of freedom, this is usually realized by considering a triple-well configuration and assuming that only a single state in each trap contributes to the dynamics. Up to now, all proposals in which the spatial adiabatic passage technique has been discussed have been effectively one dimensional: The traps are arranged in a linear geometry and a single particle in one of the outer traps is coherently transferred to the other outermost trap with very high fidelity. Significant work has been done for this process by discussing efficiency and robustness for single atoms [15,17], electrons [18], atomic vortices [19], holes [20], and BECs [21]. Proposals for spatial adiabatic passage for cold atoms propagating in systems of three coupled waveguides have also been discussed using effective one-dimensional (1D) models [22]. Recently, spatial adiabatic passage for light propagating in a system of three

coupled optical waveguides [23] has been experimentally reported.

In this work, we go beyond those well-understood 1D spatial adiabatic passage systems and focus on the possibilities offered by their extension to two dimensions. The inclusion of this degree of freedom allows considering different scenarios in which all traps can be tunnel coupled simultaneously. Contrary to the well-discussed 1D models for spatial adiabatic passage, the two-dimensional (2D) scenario has no fully equivalent model in quantum optics, where the STIRAP technique involves only two laser couplings of adjacent transitions of a three-level atomic system. Furthermore, understanding the fundamentals of 2D spatial adiabatic passage opens the possibility to study physical scenarios that require a full 2D description, such as the implementation of new interferometric schemes [24], which take advantage of the existing level crossings, or the generation of angular momentum carrying states. Angular momentum is an inherent 2D quantity, which can only be created in systems in which rotational symmetry is broken. We demonstrate that, by applying a spatial adiabatic passage sequence in a system of three traps with broken spatial symmetry, a single particle can be completely transferred from the ground vibrational state of the initial trap to the two degenerate first excited states of the final trap. Depending on the total time of the process, this can generate angular momentum with values oscillating between $\pm\hbar$. Furthermore, the process is robust since both the complete transfer and the generation of angular momentum occur within a broad range of parameter values. We model the generation of angular momentum by using the asymptotic states of the individual traps and the results are confirmed with a numerical integration of the full 2D Schrödinger equation. Note that such a two-dimensional process constitutes an alternative method to standard techniques for the generation of angular momentum in ultracold atoms [7–14].

II. PHYSICAL SYSTEM

We consider a system consisting of three 2D harmonic potentials (labeled *A*, *B*, and *C*) (see Fig. 1), where initially
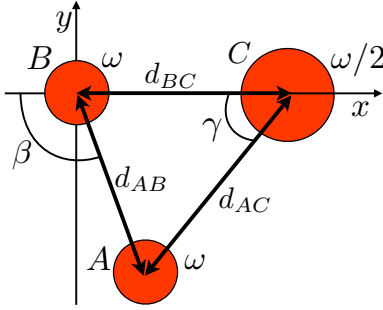
FIG. 1. (Color online) Schematic representation of the system of three harmonic traps with broken spatial symmetry. Traps A and B have a trapping frequency ω and trap C has a trapping frequency $\omega/2$.

a single particle is located in the vibrational ground state of trap A. The trapping frequencies of A and B are equal ($\omega_A = \omega_B = \omega$) and the one for C is half that value ($\omega_C = \omega/2$), so a resonance exists between the ground levels of traps A and B and the first excited level of trap C. Since the first excited energy level of trap C is double degenerate, it supports an angular momentum carrying state through a superposition of the two energy eigenstates $\psi_{1,0}^C(x,y)$ and $\psi_{0,1}^C(x,y)$ in the chosen x-y reference frame. In particular, maximum angular momentum $\langle L_z \rangle = \pm \hbar$ occurs when the two degenerate states (i) are equally populated and (ii) have a phase difference of $\pi/2$, i.e.,

$$\psi_{n=1,l=\pm 1}^C(r,\theta) = \frac{1}{\sqrt{2}}\left[\psi_{1,0}^C(x,y) \pm i\psi_{0,1}^C(x,y)\right]. \quad (1)$$

Here the $\psi_{n=1,l=\pm 1}^C(r,\theta)$ are the eigenfunctions of the first excited states of the C trap in polar coordinates, with n and l being the principal quantum number and the z component of the angular momentum, respectively.

The first thing to note is that an effective 1D configuration in which all traps are arranged in a straight line along the x axis can only lead to population transfer to the state $\psi_{1,0}^C(x,y)$ and not to the generation of angular momentum. To populate both of the degenerate states it is necessary to break the symmetry of the linear configuration and here we do this by considering geometries in which the A trap is rotated around the B trap and forms an angle β with respect to the x axis, as can be seen in Fig. 1. The positions of the trap centers are $x_A = -d_{AB}\cos\beta$, $y_A = -d_{AB}\sin\beta$, $x_B = y_B = 0$, $x_C = d_{BC}$, and $y_C = 0$, where d_{AB} and d_{BC} are the distances between the A and B and the B and C traps, respectively. In the x-y reference frame, the ground states in the A and B traps can be expressed as $\psi_{0,0}^A = \phi_0^\omega(x + d_{AB}\cos\beta)\phi_0^\omega(y + d_{AB}\sin\beta)$ and $\psi_{0,0}^B = \phi_0^\omega(x)\phi_0^\omega(y)$, respectively. For the C trap with $\omega/2$ we consider the eigenfunctions $\psi_{1,0}^C = \phi_1^{\omega/2}(x - d_{BC})\phi_0^{\omega/2}(y)$ and $\psi_{0,1}^C = \phi_0^{\omega/2}(x - d_{BC})\phi_1^{\omega/2}(y)$. Here $\phi_n^{\tilde{\omega}}$ are the single-particle eigenfunctions for the nth vibrational state of the 1D quantum harmonic oscillator with trapping frequency $\tilde{\omega}$.

The breaking of symmetry introduces two effects with respect to effective 1D configurations: (i) The traps A and C can get close enough to allow direct tunnel coupling and (ii) there is no longer a preferred direction along which one of the states in C can line up. Thus, since the position of the

A trap with respect to the C trap forms an angle γ with the x axis, there is a population transfer between states $\psi_{0,0}^A$ and $\psi_{1,0}^C$ with coupling rate $J_{1,0}^{AC}$, but also between $\psi_{0,0}^A$ and $\psi_{0,1}^C$ with coupling rate $J_{0,1}^{AC}$. Therefore, both first excited states of the C trap become involved in the dynamics of the system, which in the basis $\{\psi_{0,0}^A, \psi_{0,0}^B, \psi_{1,0}^C, \psi_{0,1}^C\}$ can be described by the 4×4 Hamiltonian

$$H = \hbar \begin{pmatrix} 0 & -J^{AB} & -J_{1,0}^{AC} & -J_{0,1}^{AC} \\ -J^{AB} & 0 & -J^{BC} & 0 \\ -J_{1,0}^{AC} & -J^{BC} & 0 & 0 \\ -J_{0,1}^{AC} & 0 & 0 & 0 \end{pmatrix}. \quad (2)$$

The coupling rates depend on the trap separation and can be calculated analytically due to the harmonicity of the potentials [15]. Additionally, the coupling rates between the ground state in A and the first excited states in C depend on the angle γ as $J_{1,0}^{AC} = J_{\omega,\omega/2}\cos\gamma$ and $J_{0,1}^{AC} = J_{\omega,\omega/2}\sin\gamma$, where $J_{\omega,\omega/2}$ is the coupling rate between the ground state of a trap with trapping frequency ω and a resonant first excited state of a trap with trapping frequency $\omega/2$. It is straightforward to check that the Hamiltonian (2) possesses four nondegenerate eigenvalues, except for $J^{BC}/\sqrt{2} = J^{AB} = J_{1,0}^{AC} = J_{0,1}^{AC}$ when two of them become degenerate.

III. GENERATION OF ANGULAR MOMENTUM CARRYING STATES

The generation of angular momentum occurs along with the transfer of the particle from the A to the C trap through a spatial adiabatic passage process [15,17]. This corresponds to a counterintuitive temporal sequence of the couplings, i.e., with the particle initially located in A and the position of B being fixed, the approach and separation sequence of the C trap towards the B trap along the x axis is initiated a time δ before the A trap approaches and separates from the B trap, keeping the angle β constant. In the following, we will analyze this process in terms of the overall energy eigenvalues and eigenstates of the system by diagonalizing the Hamiltonian in Eq. (2). To approach and separate the traps, the evolution of the distances d_{BC} and d_{AB} follows a cosine function evaluated between 0 and 2π [see Fig. 2(a), left]. The right-hand-side panel of Fig. 2(a) shows the corresponding tunneling rates and Fig. 2(b) displays the temporal evolution of all four energy eigenvalues of the Hamiltonian. Note that for the chosen parameters no level crossing occurs.

The population of each asymptotic level of the traps for the four energy eigenstates of the system is shown in Fig. 3. Since initially the particle is in the A trap, the eigenfunction of the system at $t = 0$ can be written as a superposition of the eigenstates Ψ_2 and Ψ_3 as

$$\psi(t = 0) = \frac{1}{\sqrt{2}}[\Psi_2(t = 0) + \Psi_3(t = 0)] = \psi_{0,0}^A, \quad (3)$$

where $\Psi_2(t = 0) = (\psi_{0,0}^A + \psi_{0,1}^C)/\sqrt{2}$ and $\Psi_3(t = 0) = (\psi_{0,0}^A - \psi_{0,1}^C)/\sqrt{2}$. If the process is adiabatic and level crossings are absent, this superposition of eigenstates is followed
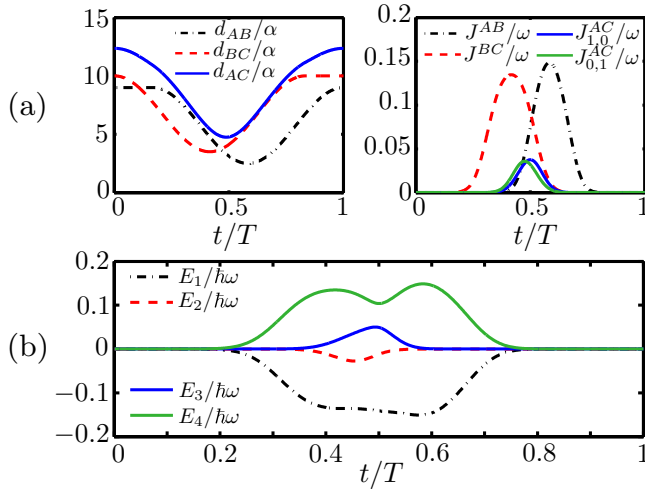
FIG. 2. (Color online) (a) Temporal evolution of the distances between traps d_{AB}, d_{BC}, and d_{AC} (left panel) and the couplings J^{AB}, J^{BC}, $J^{AC}_{1,0}$, and $J^{AC}_{0,1}$ (right panel), during the spatial adiabatic passage process. (b) Energy eigenvalues as a function of time. The parameter values are $\beta = 0.55\pi$, $\delta = 0.2T$, and d_{BC} and d_{AB} with values between 10α and 3.5α and between 9α and 2.5α, respectively, where $\alpha = \sqrt{\hbar/m\omega}$, m is the mass of the particle, and T is the total time of the process.

all through the process, leading to a final state of the form

$$\psi(t=T) = \frac{1}{\sqrt{2}} \left[\Psi_2(t=T) \exp\left(-\frac{i}{\hbar} \int_0^T E_2(t)dt\right) \right.$$
$$\left. + \Psi_3(t=T) \exp\left(-\frac{i}{\hbar} \int_0^T E_3(t)dt\right) \right]. \quad (4)$$

As it can be seen from Fig. 3, at the end of the process the eigenstates Ψ_2 and Ψ_3 only involve the asymptotic states of the C trap: $\Psi_2(t=T) = a\psi^C_{0,1} - b\psi^C_{1,0}$ and $\Psi_3(t=T) = b\psi^C_{0,1} + a\psi^C_{1,0}$, where $|a|^2 + |b|^2 = 1$. This means that by following the two eigenstates Ψ_2 and Ψ_3, a complete transfer of population from the initial trap A to the final trap C is achieved. Noting that the superpositions $(a\psi^C_{0,1} - b\psi^C_{1,0})$ and $(b\psi^C_{0,1} + a\psi^C_{1,0})$ are also two asymptotic eigenstates of the C trap in a reference frame rotated with respect to $\psi^C_{1,0}$ and $\psi^C_{0,1}$, we call them $\psi'^C_{0,1} = \Psi_2(t=T)$ and $\psi'^C_{1,0} = \Psi_3(t=T)$. It is then easy to see from Eq. (4) that $\psi'^C_{0,1}$ and $\psi'^C_{1,0}$ are equally populated and that the phase difference between them is given by

$$\varphi(t=T) = \frac{1}{\hbar} \int_0^T [E_3(t) - E_2(t)]dt. \quad (5)$$

From Fig. 2(b) it can be seen that the phase difference will be directly proportional to T since the energy difference between the energy eigenvalues E_3 and E_2 follows the same pattern, independently of the total time of the process. Rewriting Eq. (4) in polar coordinates, it is possible to show that the expected value of the angular momentum is a function of the phase difference φ,

$$\langle L_z(T) \rangle = \hbar \sin[\varphi(T)]. \quad (6)$$

Therefore, the generated angular momentum $\langle L_z \rangle$ will follow a sinusoidal curve as a function of T with a maximum

at $\varphi = (n + 1/2)\pi$ for $n \in \mathbb{N}$. We have checked that the above process works for all angles $0 < \beta < \beta_t$, which is the parameter range in which the energy eigenspectrum and eigenfunctions are similar to the ones shown in Figs. 2 and 3. The only significative variation is that the energy difference between E_3 and E_2 is smaller for smaller angles, leading to longer oscillation periods of the angular momentum as a function of T. Around $\beta_t \approx 0.625\pi$, the energy eigenstates Ψ_3 and Ψ_4 become almost degenerate at one point during the evolution, which limits the possibility to follow the superposition of the states Ψ_2 and Ψ_3 adiabatically. As discussed earlier, this particular time corresponds to the instant at which $J^{BC}/\sqrt{2} \approx J^{AB} \approx J^{AC}_{1,0} \approx J^{AC}_{0,1}$ and β_t therefore represents the angle up to which both a complete transfer and the generation of angular momentum work efficiently.

IV. NUMERICAL SIMULATIONS

Although above we used the asymptotic states of the individual traps to describe the dynamics of the system, the full dynamics is governed by the 2D Schrödinger equation

$$i\hbar \frac{\partial}{\partial t} \psi(x,y) = \left[-\frac{\hbar^2}{2m} \nabla^2 + V(x,y) \right] \psi(x,y), \quad (7)$$

where ∇^2 is the 2D Laplace operator and $V(x,y)$ is the trapping potential, which we assume to be constructed from truncated harmonic oscillator potentials

$$V(x,y) = \min_{i=A,B,C} \left\{ \frac{1}{2} m\omega_i^2 [(x - x_i)^2 + (y - y_i)^2] \right\}. \quad (8)$$

Here (x_i, y_i) with $i = A, B, C$ are the positions of the individual trap centers, $\omega_A = \omega_B = \omega$, and $\omega_C = \omega/2$. To establish the validity of our model above, we present in the following
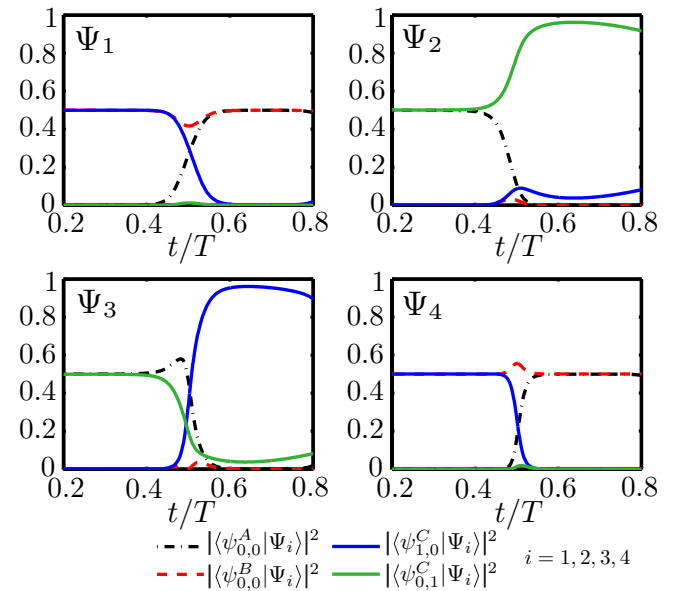

FIG. 3. (Color online) Temporal evolution of the population of each asymptotic level of the traps ($\psi^A_{0,0}$, $\psi^B_{0,0}$, $\psi^C_{1,0}$, and $\psi^C_{0,1}$) for the four eigenstates of the system (Ψ_1, Ψ_2, Ψ_3, and Ψ_4). The parameter values are the same as in Fig. 2.
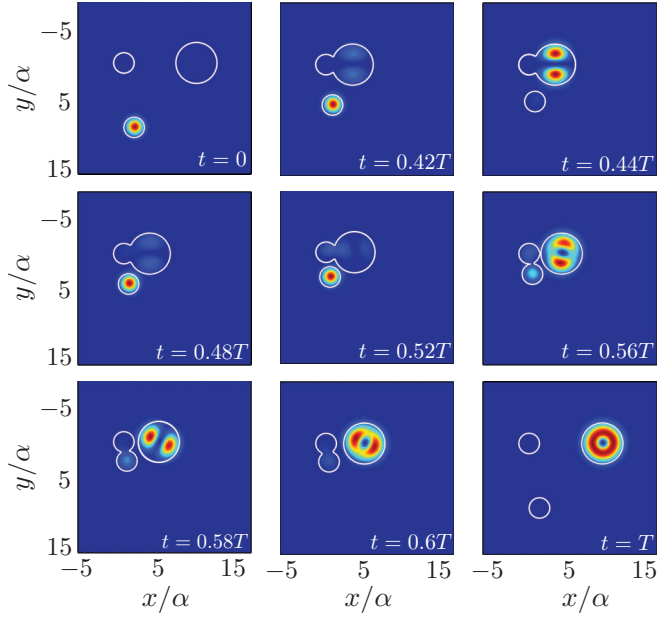
FIG. 4. (Color online) Temporal evolution of the population distribution of the single particle in the system of three traps with broken spatial symmetry for $T = 5183\omega^{-1}$ and the parameter values as in Fig. 2. The adiabatic following of the superposition of $\Psi_2(t)$ and $\Psi_3(t)$ can be observed by comparing with Fig. 3: From $t = 0.42T$ to $0.48T$ oscillations corresponding to the phase difference between $\Psi_2(t < 0.5T) = (\psi_{0,0}^A + \psi_{0,1}^C)/\sqrt{2}$ and $\Psi_3(t < 0.5T) = (\psi_{0,0}^A - \psi_{0,1}^C)/\sqrt{2}$ are shown; for $t = 0.58T$ and $0.6T$ oscillations due to the phase difference between $\Psi_2(t > 0.5T) = \psi_{0,1}'^C$ and $\Psi_3(t > 0.5T) = \psi_{1,0}'^C$ are also observed.

the numerical solution of Eq. (7), with the trapping potential Eq. (8) in the regime where $\beta < \beta_t$.

The population distribution at different times is shown in Fig. 4 for a process of total time $T = 5183\omega^{-1}$. One can see that a single particle is completely transferred from the A trap to the C trap, where a state with maximum angular momentum $\langle L_z \rangle = -\hbar$ is created, which corresponds to the adiabatic following of the eigenstates Ψ_2 and Ψ_3 (see also point c in Fig. 5).

In agreement with Eq. (6), Fig. 5 shows the sinusoidal behavior of the angular momentum generated in the C trap as a function of T, with maximum values of $\pm\hbar$. We have numerically checked that, as long as the process is performed adiabatically, both the generation of angular momentum and the complete population transfer into the C trap work efficiently over a broad range of parameter values, including different distances between the traps and angles ranging from very small values of β up to $\beta_t \approx 0.625\pi$. Thus the process is very robust and highly versatile.

Finally, let us briefly comment on a possible implementation of the above scheme using current technology. Optical microtraps, where atoms are trapped in the focal point of a red-detuned laser beam, can be used to create versatile potentials for single atoms and the presented triple-well system can, for example, be built using holographic techniques with programmable spatial light modulators [25]. This setup allows for the storage of a single atom per trap and the dynamical control of the trapping potentials, especially on time scales
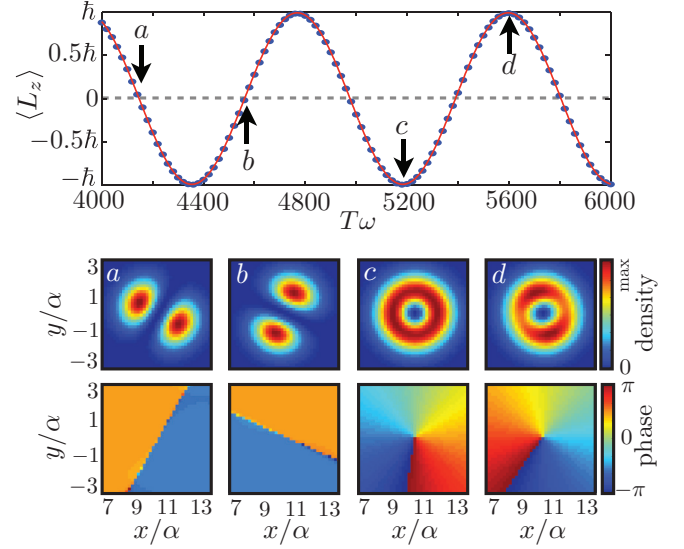

FIG. 5. (Color online) Generated angular momentum as a function of the total time of the process T (upper plot) and final states in the C trap and their phases for four different final total times a, b, c, and d (lower plots). The parameter values are the same as in Fig. 2.

required by the adiabaticity condition. Note that the process we describe can also be realized for light in three-dimensional laser-written optical waveguide arrays [26].

V. CONCLUSION

We have extended the spatial adiabatic passage technique to the 2D case, demonstrating that angular momentum can be successfully generated by breaking the symmetry of the coupling sequence in a system of three harmonic traps of different trapping frequencies. Starting with a single particle in the ground state of a harmonic trap with frequency ω, it can be fully transferred to the degenerate first excited states of a final harmonic trap of frequency $\omega/2$ by following adiabatically a superposition of two energy eigenstates of the system. The energy difference between these two eigenstates results in a phase difference between the equally populated excited states of the final harmonic trap, which leads to the generation of angular momentum. The obtained values oscillate between $\pm\hbar$ and depend on the total time of the process. We have modeled this process by using the asymptotic levels of the three harmonic traps and checked the results against the numerical solution of the full two-dimensional Schrödinger equation for a broad range of parameter values. Our work shows that adiabatic techniques for center-of-mass states hold significant potential for processes that have no direct equivalent in, for example, the control of internal degrees of freedom.

[1] C. E. Wieman, D. E. Pritchard, and D. J. Wineland, Rev. Mod. Phys. **71**, S253 (1999); A. D. Cronin, J. Schmiedmayer, and D. E. Pritchard, *ibid.* **81**, 1051 (2009); F. Schmidt-Kaler, T. Pfau, P. Schmelcher, and W. Schleich, New J. Phys. **12**, 065014 (2010); M. Lewenstein, A. Sanpera, V. Ahufinger, B. Damski, A. Sen(De), and U. Sen, Adv. Phys. **56**, 2 (2007); M. Lewenstein, A. Sanpera, and V. Ahufinger, *Ultracold Atoms in Optical Lattices: Simulating Quantum Manybody Systems* (Oxford University Press, Oxford, 2012).

[2] J. R. Abo-Shaeer, C. Raman, J. M. Vogels, and W. Ketterle, Science **292**, 476 (2001).

[3] S. Thanvanthri, K. T. Kapale, and J. P. Dowling, J. Mod. Opt. **59**, 1180 (2012).

[4] K. T. Kapale and J. P. Dowling, Phys. Rev. Lett. **95**, 173601 (2005); S. Thanvanthri, K. T. Kapale, and J. P. Dowling, Phys. Rev. A **77**, 053825 (2008).

[5] N. Lo Gullo, S. McEndoo, Th. Busch, and M. Paternostro, Phys. Rev. A **81**, 053625 (2010).

[6] Y. Castin, Z. Hadzibabic, S. Stock, J. Dalibard, and S. Stringari, Phys. Rev. Lett. **96**, 040405 (2006).

[7] B. Jackson, J. F. McCann, and C. S. Adams, Phys. Rev. Lett. **80**, 3903 (1998).

[8] A. E. Leanhardt, A. Gorlitz, A. P. Chikkatur, D. Kielpinski, Y. Shin, D. E. Pritchard, and W. Ketterle, Phys. Rev. Lett. **89**, 190403 (2002); L. Dobrek, M. Gajda, M. Lewenstein, K. Sengstock, G. Birkl, and W. Ertmer, Phys. Rev. A **60**, R3381 (1999).

[9] K.-P. Marzlin, W. Zhang, and E. M. Wright, Phys. Rev. Lett. **79**, 4728 (1997); G. Nandi, R. Walser, and W. P. Schleich, Phys. Rev. A **69**, 063606 (2004); M. F. Andersen, C. Ryu, P. Clade, V. Natarajan, A. Vaziri, K. Helmerson, and W. D. Phillips, Phys. Rev. Lett. **97**, 170406 (2006).

[10] A. Muthukrishnan and C. R. Stroud, Jr., J. Opt. B **4**, S73 (2002).

[11] J. E. Williams and M. J. Holland, Nature (London) **401**, 568 (1999); K. W. Madison, F. Chevy, W. Wohlleben, and J. Dalibard, Phys. Rev. Lett. **84**, 806 (2000); P. C. Haljan, I. Coddington, P. Engels, and E. A. Cornell, **87**, 210403 (2001).

[12] S. Inouye, S. Gupta, T. Rosenband, A. P. Chikkatur, A. Gorlitz, T. L. Gustavson, A. E. Leanhardt, D. E. Pritchard, and W. Ketterle, Phys. Rev. Lett. **87**, 080402 (2001).

[13] B. P. Anderson, P. C. Haljan, C. A. Regal, D. L. Feder, L. A. Collins, C. W. Clark, and E. A. Cornell, Phys. Rev. Lett. **86**, 2926 (2001).

[14] D. R. Scherer, C. N. Weiler, T. W. Neely, and B. P. Anderson, Phys. Rev. Lett. **98**, 110402 (2007).

[15] K. Eckert, M. Lewenstein, R. Corbalan, G. Birkl, W. Ertmer, and J. Mompart, Phys. Rev. A **70**, 023606 (2004).

[16] K. Bergmann, H. Theuer, and B. W. Shore, Rev. Mod. Phys. **70**, 1003 (1998).

[17] T. Opatrný and K. K. Das, Phys. Rev. A **79**, 012113 (2009); T. Morgan, B. O'Sullivan, and Th. Busch, *ibid.* **83**, 053620 (2011); Yu. Loiko, V. Ahufinger, R. Corbalán, G. Birkl, and J. Mompart, *ibid.* **83**, 033629 (2011); A. Benseny, J. Bagudà, X. Oriols, and J. Mompart, *ibid.* **85**, 053619 (2012).

[18] A. D. Greentree, J. H. Cole, A. R. Hamilton, and Lloyd C. L. Hollenberg, Phys. Rev. B **70**, 235317 (2004).

[19] S. McEndoo, S. Croke, J. Brophy, and Th. Busch, Phys. Rev. A **81**, 043640 (2010).

[20] A. Benseny, S. Fernandez-Vidal, J. Baguda, R. Corbalan, A. Picon, L. Roso, G. Birkl, and J. Mompart, Phys. Rev. A **82**, 013604 (2010).

[21] E. M. Graefe, H. J. Korsch, and D. Witthaut, Phys. Rev. A **73**, 013617 (2006); M. Rab, J. H. Cole, N. G. Parker, A. D. Greentree, L. C. L. Hollenberg, and A. M. Martin, *ibid.* **77**, 061602(R) (2008); J. H. Cole, A. D. Greentree, L. C. L. Hollenberg, and S. Das Sarma, Phys. Rev. B **77**, 235418 (2008); C. Ottaviani, V. Ahufinger, R. Corbalán, and J. Mompart, Phys. Rev. A **81**, 043621 (2010).

[22] K. Eckert, J. Mompart, R. Corbalán, M. Lewenstein, and G. Birkl, Opt. Commun. **264**, 264 (2006); B. O'Sullivan, P. Morrissey, T. Morgan, and Th. Busch, Phys. Scr. **T140**, 014029 (2010); T. Morgan, L. J. O'Riordan, N. Crowley, B. O'Sullivan, and Th. Busch, Phys. Rev. A **88**, 053618 (2013).

[23] S. Longhi, G. Della Valle, M. Ornigotti, and P. Laporta, Phys. Rev. B **76**, 201101 (2007); R. Menchon-Enrich, A. Llobera, V. J. Cadarso, J. Mompart, and V. Ahufinger, IEEE Photon. Tech. Lett. **24**, 536 (2012); R. Menchon-Enrich, A. Llobera, J. Vila-Planas, V. J. Cadarso, J. Mompart, and V. Ahufinger, Light Sci. Appl. **2**, e90 (2013).

[24] R. Menchon-Enrich, S. McEndoo, Th. Busch, V. Ahufinger, and J. Mompart, arXiv:1401.6072 [quant-ph] (2014).

[25] S. Bergamini, B. Darquie, M. Jones, L. Jacubowiez, A. Browaeys, and P. Grangier, J. Opt. Soc. Am. B **21**, 1889 (2004).

[26] G. D. Marshall, A. Politi, J. C. F. Matthews, P. Dekker, M. Ams, M. J. Withford, and J. L. O'Brien, Opt. Express **17**, 12546 (2009).